ORNL/TM-13525

ornl

OAK RIDGE
NATIONAL
LABORATORY

LOCKHEED MARTIN

Doppler Broadening Revisited

N. M. Larson
M. C. Moxon
L. C. Leal
H. Derrien

MANAGED AND OPERATED BY
LOCKHEED MARTIN ENERGY RESEARCH CORPORATION
FOR THE UNITED STATES
DEPARTMENT OF ENERGY

ORNL-27 (3-96)

ORNL/TM-13525

Computational Physics and Engineering Division

Doppler Broadening Revisited

N. M. Larson, M. C. Moxon, L. C. Leal, H. Derrien
Oak Ridge National Laboratory

Date Published: January 1998

Prepared by the
OAK RIDGE NATIONAL LABORATORY
managed by
LOCKHEED MARTIN ENERGY RESEARCH
for the
U.S. DEPARTMENT OF ENERGY
under contract DE-AC05-96OR22464

CONTENTS

LIST OF FIGURES

ACKNOWLEDGMENTS

This work was sponsored by the U.S. Department of Energy (DOE), under contract DE-AC05-84OR21400 with Lockheed Martin Energy Research. The authors are particularly indebted to D. Cabrilla, Environmental Management, U.S. Department of Energy, Washington, D.C., for his support.

ABSTRACT

The use of the high-energy Gaussian approximation to the free gas model of Doppler broadening has a long and distinguished history, dating back to early computer days when ψ and χ functions provided the most accurate computations available. In today's computing environment, however, use of the high-energy approximation is no longer necessary, and may lead to erroneous results. In this paper a derivation of the free gas model is presented, and the high-energy approximation derived from that. Differences between the two models are examined both analytically and via computations. Because the differences are visible (albeit not necessarily of significance in many cases), the authors recommend against continued use of the high-energy Gaussian approximation.

1. INTRODUCTION

Early in October of 1996, Mick Moxon and Herve Derrien began extended visits at Oak Ridge National Laboratory, working with L. Leal and N. Larson on various aspects of resonance parameter analysis. A major purpose of Moxon's visit was to facilitate comparisons between the two cross section analysis codes REFIT [MO77, MO91] and SAMMY [LA96], both in general and with particular emphasis on the ^{235}U analysis. As part of the comparison effort, REFIT and SAMMY calculations were made, first of the unbroadened ^{235}U cross sections and next of the Doppler-broadened cross sections, using parameters of the recent analysis of Leal, Derrien, and Larson [LE97]. Preliminary results are as follows:

For the unbroadened calculations, so long as all input parameters and all physical constants are given the exact same values for both codes, theoretical cross sections produced by the codes are equivalent to within 1 part in 10^6 (with certain exceptions). Detailed code comparison results will be described in another report [LA98].

During the course of the calculation minor glitches were found and fixed in each of the codes. In SAMMY, a too-short cutoff in the integration limits for the Doppler broadening was found to produce a slight discontinuity in the Doppler-broadened values at about 3.5 Doppler widths either side of a narrow resonance. In REFIT, a line of coding designed to prevent divide overflows when successive grid points were too close together led to miscalculation of the Doppler-broadened cross section for resonances with widths less than ~ 15 meV. For both codes the location and density of grid points used in the numerical integration schemes have been reconsidered and slightly restructured to optimize the calculations.

It is not the purpose of this paper to discuss either the details of the comparison nor any modifications made to the ^{235}U resonance parameter set as a result of this effort; rather, in this report we will concentrate on observations related to the Doppler broadening calculation.

Toward this end the remainder of this report is organized as follows: In Sect. 2 we present a derivation of the free gas model of Doppler broadening (sometimes referred to as the "ideal gas model"), and of the high-energy Gaussian approximation to the free gas model. In Sect. 3 the case of very narrow resonances is considered, first theoretically (assuming delta-function resonances) and then computationally. The Doppler broadening of various other energy-dependent cross sections is discussed in Sect. 4. A summary of results is presented in Sect. 5.

2. DERIVATION OF DOPPLER BROADENING EQUATIONS

The following is a quote (with notational changes for convenience) from Fritz Froehner's definitive paper "Applied Neutron Resonance Theory" [FR89]; comments in square brackets are added by the authors of this paper.

$$= \frac{1}{\pi^{3/2} u^3} \int_0^{2\pi} d\phi \int_0^{\infty} dw\, w^3 \sigma\left(\frac{mw^2}{2}\right) \exp\left(-\frac{(v^2+w^2)}{u^2}\right) \int_{-1}^{+1} d\mu\, \exp\left(-\frac{2vw\mu}{u^2}\right)$$

$$= \frac{2\pi}{\pi^{3/2} u^3} \int_0^{\infty} dw\, w^3 \sigma\left(\frac{mw^2}{2}\right) \exp\left(-\frac{(v^2+w^2)}{u^2}\right)\left(\frac{-u^2}{2vw}\right)\left[\exp\left(-\frac{2vw}{u^2}\right) - \exp\left(+\frac{2vw}{u^2}\right)\right]$$

$$= \frac{1}{v\sqrt{\pi}\, u} \int_0^{\infty} dw\, w^2 \sigma\left(\frac{mw^2}{2}\right)\left[\exp\left(-\frac{(v-w)^2}{u^2}\right) - \exp\left(-\frac{(v+w)^2}{u^2}\right)\right] . \tag{4}$$

[This equation may be more familiar to most users when written as the sum of two integrals,

$$\bar{\sigma}\left(E = \frac{mv^2}{2}\right) = \frac{1}{v^2\sqrt{\pi}\, u} \int_0^{\infty} dw\, w^2 \sigma\left(\frac{mw^2}{2}\right) \exp\left(-\frac{(v-w)^2}{u^2}\right) - \frac{1}{v^2\sqrt{\pi}\, u} \int_0^{\infty} dw\, w^2 \sigma\left(\frac{mw^2}{2}\right) \exp\left(-\frac{(v+w)^2}{u^2}\right) . \tag{5}$$

At sufficiently high energies, the contribution from the second integral may be omitted since the value of the exponential is vanishingly small.]

To simplify Eq. (4) further, we make the following **definition**:

$$\begin{aligned} s(w) &= \sigma(\, m(w)^2/2) \quad \text{for } w > 0 \\ &= -\sigma(m(-w)^2/2) \quad \text{for } w < 0 . \end{aligned} \tag{6}$$

Equation (4) then becomes

$$\bar{\sigma}\left(\frac{mv^2}{2}\right) = \frac{1}{v^2\sqrt{\pi}\, u} \int_{-\infty}^{\infty} dw\, w^2 s(w) \exp\left(-\frac{(v-w)^2}{u^2}\right) . \tag{7}$$

For programming convenience, we make a change of variable from velocity to square root of energy. Thus instead of v we use

$$V = \sqrt{E} = v\sqrt{m/2} \;; \tag{8}$$

we redefine W to be

$$W = w\sqrt{m/2} \;, \tag{9}$$

and define U as

$$U = \sqrt{m/2}\, u = \sqrt{mkT/M} \;. \tag{10}$$

note that this quantity is energy-dependent. Expanding the integrand of Eq. (13) in powers of $(E-E')$, and keeping only first-order terms, give a value of 1 for the ratio E'/E, and $E - E - (E-E')/2 = (E-E')/2$ for the quantity in the exponential. Thus the HEGA becomes

$$\bar{\sigma}_{HEGA}(E) \cong \frac{1}{\sqrt{\pi}\,\Delta} \int_{Emin}^{\infty} dE' \; \sigma(E') \exp\left(-\frac{(E-E')^2}{\Delta^2}\right) \quad . \tag{15}$$

Extending the lower limit to negative infinity (since that portion of the integrand is essentially zero) then gives the usual Gaussian formulation of the free gas model.

3. VERY NARROW RESONANCES

3.1. THEORETICAL DERIVATION FOR DELTA-FUNCTION RESONANCE

In order to understand whether HEGA might differ from FGM even at high energies, consider first the case of an isolated narrow resonance. For illustrative purposes the cross section is taken to be a delta-function of the form

$$\sigma(E') = \delta(E' - E_0) \quad . \tag{16}$$

With this value for the cross section, the HEGA-broadened cross section is found directly from Eq. (15):

$$\bar{\sigma}_{HEGA}(E) = \frac{1}{\sqrt{\pi}\,\Delta} \exp\left(-\frac{(E-E_0)^2}{\Delta^2}\right) = \frac{1}{\sqrt{\pi}\,2\,U\,V} \exp\left(-\frac{(V^2-V_0^2)^2}{4\,V^2\,U^2}\right) \quad , \tag{17}$$

in which the energy-variables have been translated to square-root-of-energy variables for ease of comparison with the FGM, and E_0 is set equal to V_0^2. To evaluate the FGM cross section, the integration variable W in Eq. (11) is first replaced by variable $E' = W^2$, so that

$$\begin{aligned} \bar{\sigma}_{FGM}(E) &= \frac{1}{V^2\sqrt{\pi}\,U} \int_{-\infty}^{\infty} \frac{dE'}{2\sqrt{E'}} \, E' \, \delta(E'-E_0) \exp\left(-\frac{\left(V-\sqrt{E'}\right)^2}{U^2}\right) \\ &= \frac{1}{V^2\sqrt{\pi}\,U} \frac{\sqrt{E_0}}{2} \exp\left(-\frac{\left(V-\sqrt{E_0}\right)^2}{U^2}\right) = \frac{1}{\sqrt{\pi}\,2\,U\,V} \frac{V_0}{V} \exp\left(-\frac{\left(V-V_0\right)^2}{U^2}\right) \quad . \end{aligned} \tag{18}$$

3.2. CALCULATIONS

To verify the results described above for delta-function resonances, calculations were performed with SAMMY using an invented element of mass 10.000 amu, ground state spin 0, with 12 s-wave resonances located at energies (in eV) of 0.25, 0.5, 1.0, 2.0, 5.0, 10.0, 20.0, 50.0, 100.0, 200.0, 500.0, and 1000.0. The radiation width for each resonance was set at 1.0 meV, and the neutron width and two fission widths for each resonance were 0.5 meV. This "element" was designated "resium" by John Story [ST81].

The same calculations have also been performed with REFIT, as well as with the codes NJOY [MA94] and MULTIPOLE [HW87]; results will be reported elsewhere [LA98].

Figure 1 shows the FGM and the HEGA for the resonance at 1 eV. Differences between the two are clearly visible on the plot. Fig. 2 gives the ratio of FGM to HEGA for the energy range from ~10^{-4} to 1.2 keV. As expected, the magnitude of this ratio becomes closer to unity as energy increases; nevertheless the differences between the two methods are still quite pronounced even for the 20-eV resonance.

Careful examination shows that physical resonances exhibit the same kinds of behavior, although for most resonances the differences between HEGA and FGM are smaller than the experimental uncertainties. One example is given in Fig. 3a, which represents a small portion of the ^{235}U fission cross section; Fig. 3b shows the resonance (doublet) near 8.8 eV. The calculated HEGA and FGM curves for the uppermost portion of this peak have been redrawn in Fig. 4 (with a dense grid, to ensure that the picture is visually smooth).

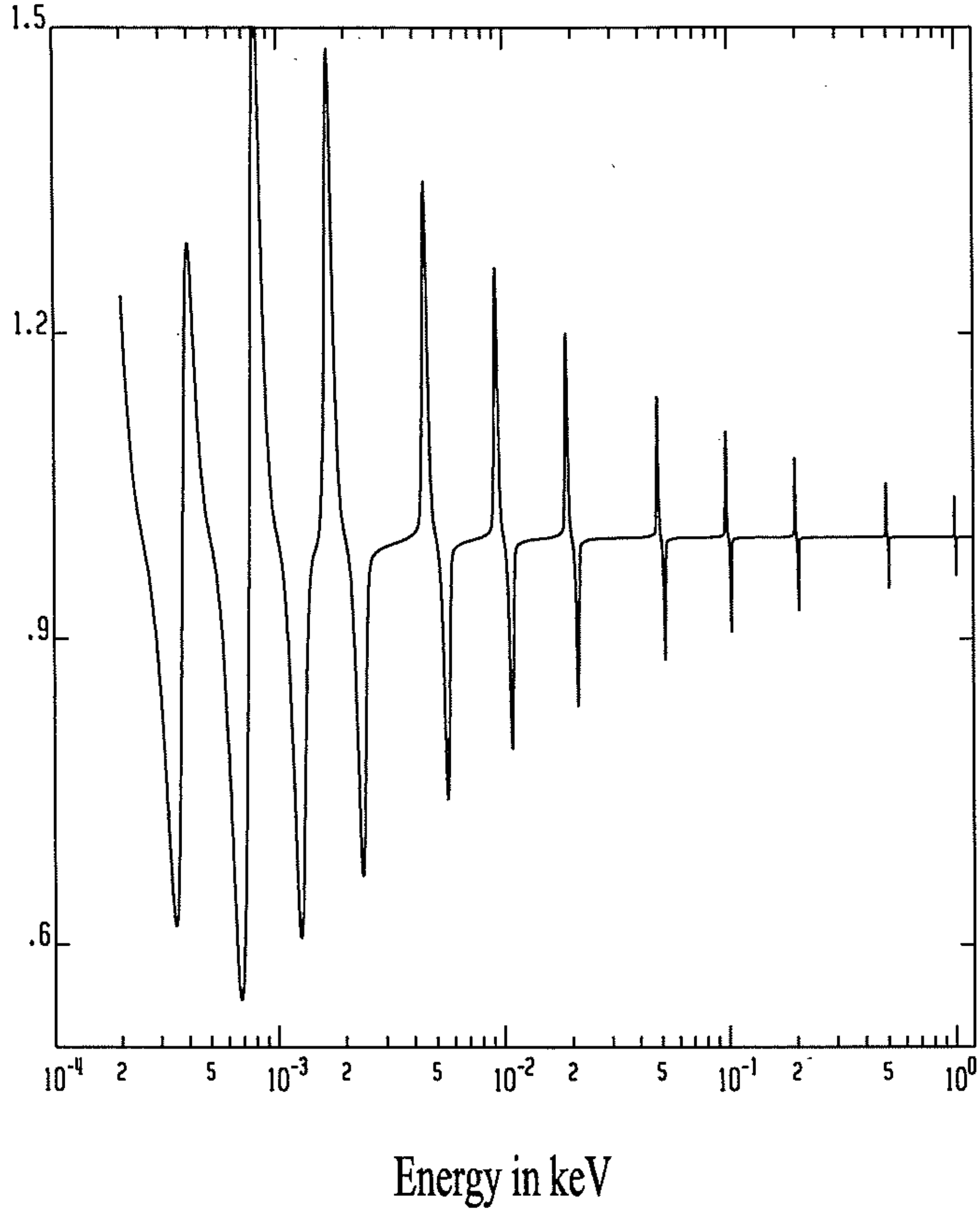

Figure 2. Ratio of the Doppler broadened capture cross section for Resium using the free gas model to that obtained using the high energy Gaussian approximation.

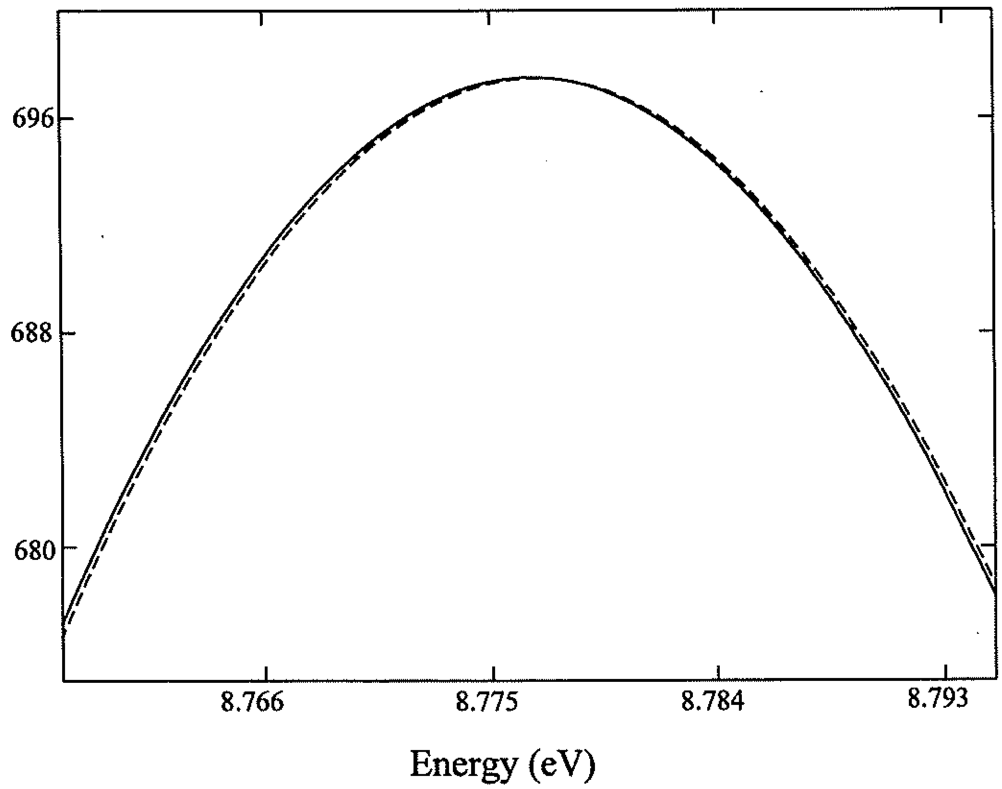

Figure 4. Calculated FGM (solid) and HEGA (dashed) curves for the peak at 8.8 eV.

4.2. DOPPLER BROADENING OF A CONSTANT CROSS SECTION.

In contrast to the $1/v$ cross section, a constant cross section is not conserved under Doppler broadening. That is is true experimentally can be seen by examining very low energy capture cross sections, for which the unbroadened cross section is constant (which can be shown by taking the low-energy limit of the Reich-Moore equations, e.g.) but the experimental cross section rises with decreasing energy. See, for example, the S elastic cross section from 0.01 to 1.0 eV or the Cu elastic cross section below 2.0 eV (on pages 100 and 234, respectively, of [VM88]), which clearly rise with decreasing energy.

To calculate analytically what effect FGM and HEGA broadening have upon a constant cross section, we first note that a constant cross section can be expressed as

$$\sigma(E) = \sigma_0 \quad . \tag{27}$$

The function S needed for our formulation of FGM broadening (see Eq. (10)) is found to be

$$\begin{aligned} S(W) &= \sigma_0 \quad \text{for } W \geq 0 \\ &= -\sigma_0 \quad \text{for } W < 0 \quad , \end{aligned} \tag{28}$$

so that Eq. (11) gives, for the FGM-broadened constant cross section,

$$\bar{\sigma}(V^2) = \frac{\sigma_0}{V^2 \sqrt{\pi}\, U} \left[\int_0^\infty dW\, W^2\, e^{-(V-W)^2/U^2} - \int_{-\infty}^0 dW\, W^2\, e^{-(V-W)^2/U^2} \right] . \tag{29}$$

Replacing $(W\text{-}V) / U$ by x gives

$$\begin{aligned} \bar{\sigma}(V^2) &= \frac{\sigma_0\, U^3}{V^2 \sqrt{\pi}\, U} \left[\int_{-v}^{\infty} dx\, (x^2 + 2xv + v^2)\, e^{-x^2} - \int_{-\infty}^{-v} dx\, (x^2 + 2xv + v^2)\, e^{-x^2} \right] \\ &= \frac{\sigma_0}{v^2 \sqrt{\pi}} \left[\int_0^\infty + \int_{-v}^0 - \int_{-\infty}^0 + \int_{-v}^0 \right] dx\, (x^2 + 2xv + v^2)\, e^{-x^2} \end{aligned}$$

$$\bar{\sigma}_{HEGA}(E) = \frac{\sigma_0}{\sqrt{\pi}\,\Delta} \int_{-\infty}^{\infty} dE' \; e^{-(E-E')^2/\Delta^2} = \sigma_0 \quad ; \qquad (33)$$

that is, the Gaussian kernel is normalized to unity, as expected. This result, which may intuitively appear to be correct, is nevertheless unphysical. As discussed above, It is well known that measured (and therefore Doppler-broadened) cross sections exhibit $1/v$ behavior at very low energies.

5. SUMMARY

The free gas model of Doppler broadening appears to be a reasonable approximation for most solid samples for neutron energy above a few tens of eV, where solid state effects can be neglected. One of the problems is the determination of the effective temperature of the sample, which should be obtained from Lamb equation (LA39) relating the effective temperature to the Debye temperature and to the actual temperature of the sample. The Debye temperature is not always well known, and most experimenters have not monitored the sample temperature during measurement, particularly for measurements performed with samples at low temperature (e.g.,liquid nitrogen temperature). Consequently the effective temperature should be one of the variables to be determined in the fit; both SAMMY and REFIT permit this option.

In this paper we have described comparisons, both theoretical and computational, of Doppler broadening using the "exact" free gas model vs. Doppler broadening using the customary high-energy Gaussian approximation. These comparisons indicate clearly that the approximate formulation does not provide an accurate representation of the exact free gas model, even for relatively high energies. While differences between the exact and the approximate models are generally small for physical resonances, nevertheless those differences do persist at all energies.

Early codes for resonance analysis and evaluation generally used the Gaussian approximation, because the ψ and χ functions (results of the convolution of the Gaussian function and the Breit-Wigner shape of the resonances) were well known and tabulated (saving computer time and space). Today, more sophisticated (and more accurate) formalisms are used for the calculation of the cross sections; the ψ and χ functions cannot be used for the Doppler broadening with these formalisms. Hence, there is no longer any computational advantage to using the Gaussian approximation.

Use of the approximate HEGA model (the high-energy Gaussian approximation) is therefore discouraged.

APPENDIX. POSITION OF PEAK OF DOPPLER-BROADENED CROSS SECTION

The HEGA- and FGM-broadened cross sections for very narrow (delta-function) resonances were discussed in Sect. 3.1 of this report; exact expressions for the two quantities are shown in Eqs. (16) and (17) respectively. In this appendix we derive the expressions for the exact energy-value of the peak cross section, where "peak" is assumed to mean "highest value of the function." This location occurs at that energy (or, equivalently, that value of V) at which the derivative of the function is zero.

For the HEGA cross section, the derivative of Eq. (16) with respect to "velocity" V is given by

$$\frac{\partial}{\partial V}\bar{\sigma}_{HEGA} = \bar{\sigma}_{HEGA} \times \left(-\frac{1}{V} - \frac{2V\,2(V^2-V_0^2)}{4V^2U^2} - \frac{2}{V}\frac{(V^2-V_0^2)^2}{4V^2U^2} \right)$$

$$= -\frac{\bar{\sigma}_{HEGA}}{2V^3U^2}\left(V^4+2V^2U^2-V_0^4\right) \quad . \tag{A.1}$$

Let $E_{Hp} = V_{Hp}^2$ represent the position of the peak. Setting the derivative in Eq. (A.1) equal to zero gives

$$V_{Hp}^4 + 2V_{Hp}^2U^2 - V_0^4 = 0 \quad , \tag{A.2}$$

which has the solution

$$E_{Hp} = V_{Hp}^2 = \sqrt{V_0^4+U^4} - U^2 \quad . \tag{A.3}$$

To simplify this equation a bit more, variable X is defined as

$$X = U^2/V_0^2 \quad ; \tag{A.4}$$

with this definition Eq. (A.3) takes the form

$$Y_H = E_{Hp}/V_0^2 = E_{Hp}/E_0 = \sqrt{1+X^2} - X \quad , \tag{A.5}$$

in which Y_H is defined as the ratio shown.

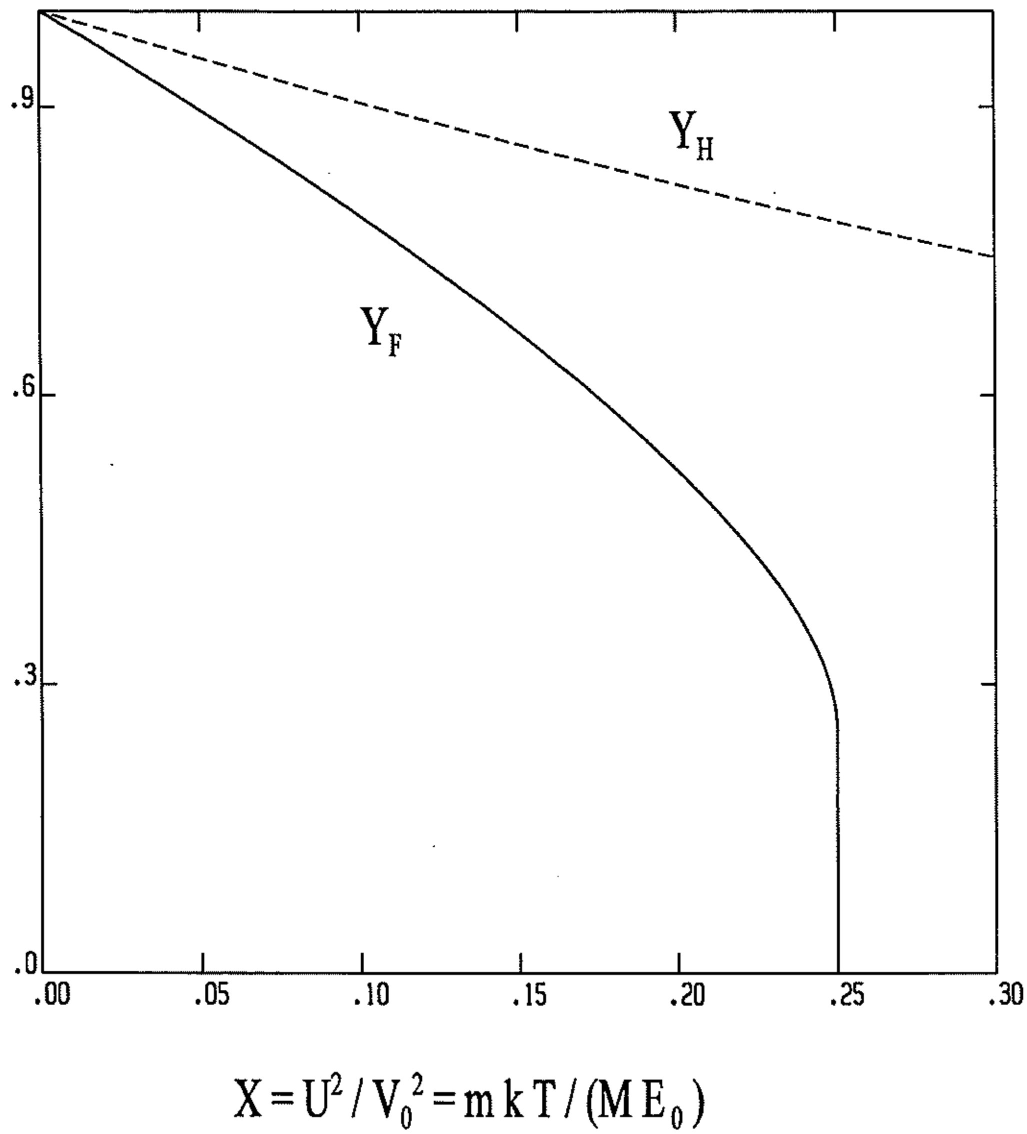

Fig. A1. Relative peak position for the Doppler-broadened delta-function cross section as a function of temperature. The solid curve shows the free gas model, and the dashed the high-energy Gaussian approximation.

INTERNAL DISTRIBUTION

1. B. L. Broadhead
2-7. H. Derrien
8. F. C. Difilippo
9. C. Y. Fu
10. N. M. Greene
11. K. Guber
12. J. A. Harvey
13. C. M. Hopper
14. D. T. Ingersoll
15. P. E. Koehler
16. M. A. Kuliasha
17. D. C. Larson
18-22. N. M. Larson
23-27. L. C. Leal
28. C. V. Parks
29. R. W. Roussin
30. C. H. Shappert
31. M. S. Smith
32. R. R. Spencer
33. R. M. Westfall
34. J. E. White
35. R. Q. Wright
36. RSICC
37-38. Laboratory Records for submission to OSTI
39. Laboratory Records, ORNL-RC
40. Central Research Library

EXTERNAL DISTRIBUTION

41. P. Blaise, DER/SPRC/LEPH, Batiment 230, Centre d'Etudes de CADARACHE, 13108 Saint Paul-lez-Durance, France
42. R. Block, Gaerttner LINAC Laboratory, Department of Environmental and Energy Engineering, Rensselaer Polytechnic Institute, Troy, NY 12180-3590
43. O. Bouland, DER/SPRC/LEPH, Batiment 230, Centre d'Etudes de CADARACHE, 13108 Saint Paul-lez-Durance, France
44. J. Burke, Gaerttner LINAC Laboratory, Department of Environmental and Energy Engineering, Rensselaer Polytechnic Institute, Troy, NY 12180-3590
45. D. Cabrilla, U.S. Department of Energy, EM-66, Clover Leaf, Room 1199, 19901 Germantown Road, Germantown, MD 20874-1290
46. D. E. Carlson, Reactor and Plant System Branch, Division of System Research, Office of Nuclear Regulatory Research, U.S. Nuclear Regulatory Commission, MS T-10 G6, RM T-10, I7, Washington, DC 20555-0001
47. F. Corvi, Central Bureau for Nuclear Measurements, Steenweg op Retie, 2240 Geel, Belgium
48. D. E. Cullen, MS L-298, Lawrence Livermore National Laboratory, P. O. Box 808, Livermore, CA 94550
49. Y. Danon, Physics Department, NRCN, P. O Box 9001, Beer-Sheva 84190, Israel
50. R. L. Dintaman, U.S. Department of Energy, DP-13, Washington, DC 20585
51. C. Dunford, Bldg 197D, National Nuclear Data Center, Brookhaven National Laboratory, Upton, NY 11973
52. J. R. Felty, U.S. Department of Energy, DP-311, Washington DC 20585
53. P. Finck, Argonne National Laboratory, Reactor Analysis Division, Bldg 208, Argonne, IL 60439
54. E. Fort, DER/SPRC/LEPH, Batiment 230, Centre d'Etudes de CADARACHE, 13108 Saint Paul-lez-Durance, France
55. C. M. Frankle, NIS-6, MS J562, Los Alamos National Laboratory, Los Alamos, NM 87545
56. S. C. Frankle, X-TM, MS B226, Los Alamos National Laboratory, Los Alamos, NM 87545
57. F. Froehner, Kernforschungszentrum Karlsruhe, Institut f. Neutronenphysik und Reacktortechnik, Postfach 336 40, D-76021 Karlsruhe, Germany
58. W. Furman, Frank Laboratory of Neutron Physics, JINR, Dubna, Russia